PHYSICAL REVIEW B VOLUME 58, NUMBER 22 1 DECEMBER 1998-II

Phonon spectrum of *B*2-FeAl: *Ab initio* calculation and comparison with data from inelastic neutron scattering

B. Meyer, V. Schott, and M. Fähnle
Max-Planck-Institut für Metallforschung, Heisenbergstrasse 1, D-70569 Stuttgart, Germany
(Received 19 August 1998)

The phonon-dispersion curves of stoichiometric *B*2-FeAl are calculated by frozen-phonon calculations and by the *ab initio* force-constant method within the framework of the density-functional theory in local density approximation and the *ab initio* mixed-basis pseudopotential method. The results are compared with experimental data obtained by inelastic neutron-scattering experiments. There are no strong anomalies in the phonon spectrum which could assist the diffusion of vacancies.
[S0163-1829(98)50446-8]

In ordered intermetallic compounds various physical quantities which are important for the technological application may or may not be influenced by lattice vibrations. For instance, it has been assumed[1] that there is a considerable effect of the vibrational entropy on the order-disorder transition, but *ab initio* computations[2] have thrown some doubt on this assumption at least for the case of Ni_3Al. Second, the phonon spectrum can be used to obtain information on migration barriers for nearest-neighbor vacancy jumps within the framework of the theory of Schober *et al.*[3] In this context, it is sometimes discussed whether the large diffusivities of some intermetallics originate from low-energy phonon modes which assist the defect migration. Indeed, inelastic neutron-scattering experiments[4] on iron-rich Fe-Si compounds with DO_3 structure revealed transverse acoustic phonon branches which are very low in energy, indicating low migration barriers, but there was no visible composition dependence and therefore the vibrational properties cannot explain the pronounced change of diffusivity with composition. In contrast, it is well known that the defect formation entropies may have a strong influence on the concentration of atomic defects well below the order-disorder transition, e.g., in *B*2-FeAl.[5] To calculate the defect formation entropies one has to determine the phonon spectra of the material with and without the considered defect. This has been done within the framework of the *ab initio* electron theory for the case of Li,[6] Na, and K,[6,7] but corresponding calculations for intermetallic compounds are lacking. Finally, the phonon spectra are required to investigate structural phase transitions within the framework of the harmonic approximation (see, e.g., Ref. 8).

The present paper represents a first step towards the above-discussed objectives for the case of intermetallic compounds which very often contain *3d* transition-metal atoms. It is shown exemplarily for the case of *B*2-FeAl that the *ab initio* electron theory in local density approximation is able to yield highly accurate phonon spectra for such systems. As a by-product, the calculation serves to explore whether there are peculiarities in the phonon spectrum of *B*2-FeAl which may assist the defect migration. To our knowledge, Ni_3Al (Ref. 2) and FeAl studied in this paper are the only examples for the *ab initio* calculation of phonon spectra in systems containing *3d* transition-metal atoms.

The calculations were performed within the framework of the *direct approach*[9–12] which is the alternative to the *linear response approach*;[13] for a short review see Ref. 9. There are two versions of the direct approach. In the frozen-phonon calculation,[12] the total energy is evaluated for a system with a displacement pattern according to a snapshot of the atom movement, and from the energy as a function of the displacement amplitude the phonon frequency is obtained. The strength of the frozen-phonon calculations is that they include automatically and exactly all the couplings between the various atoms which are relevant for the respective phonon mode. The disadvantage is that they are restricted to wave vectors for which the phonon displacement pattern is commensurate to the supercells used in the calculations, i.e., only short-wavelength phonons can be considered for reasonable supercell sizes. In the following we therefore use the frozen-phonon calculations just for convergence tests and for a check of the results obtained by the second variant of the direct method, the direct force-constant approach. In this latter approach, single atoms in the infinite crystal are displaced, and the resulting forces on all the other atoms are calculated. From these forces the elements of the force-constant matrix are obtained, the dynamical matrix is determined from the force-constant matrix by Fourier transformation, and the phonon frequencies are calculated by a diagonalization of the dynamical matrix (for details, see Refs. 9–11). The advantage of the force-constant approach is that phonon frequencies for arbitrary wave vectors can be considered which allows the determination of the phonon density of states. The disadvantage is that in a practical calculation only a restricted number of force constants can be obtained so that the dynamical matrix can be calculated only approximately. This represents the main limitation of the approach and will be discussed in the following.

Suppose that the calculational method yields the true force constants $\underline{\underline{\Phi}}_{\alpha,\alpha'}(\mathbf{T}')$ between the basis atoms α in the elementary unit cell at $\mathbf{T}=0$ and the atoms α' in the elementary unit cell with translation vector $\mathbf{T}'$. Then the dynamical matrix is given by

$$\underline{\underline{D}}_{\alpha,\alpha'}(\mathbf{q}) = \sum_{\mathbf{T}'} \frac{1}{\sqrt{M_\alpha M_{\alpha'}}} \underline{\underline{\Phi}}_{\alpha,\alpha'}(\mathbf{T}')\, e^{i\mathbf{q}\mathbf{T}'}, \qquad (1)$$

where M_α is the mass of the basis atom α and $\mathbf{q}$ denotes the wave vector of the phonon. Of course, in a practical calculation only a finite number of coupling constants can be obtained and used for the calculation of the dynamical matrix (truncated dynamical matrix). Furthermore, many of the methods used for the calculation of the force constants are based on a reciprocal space formalism. Then—instead of displacing a single atom in an infinitely extended system—a supercell containing many elementary unit cells is constructed and a single atom of the supercell is displaced. Because the supercells then are repeated periodically, there is a periodic array of displaced atoms, and the force on a considered atom is given by a superposition of the forces exerted by all the displaced atoms on the considered atom. The force constants between the atoms in the supercell calculated from these forces therefore represent effective force constants

$$\underline{\underline{\Phi}}^{eff}_{\alpha,\alpha'}(\mathbf{T}^{ec}) = \sum_{\mathbf{T}^{sc}} \underline{\underline{\Phi}}_{\alpha,\alpha'}(\mathbf{T}^{sc}+\mathbf{T}^{ec}), \tag{2}$$

where we have composed the translation vector $\mathbf{T}$ by a translation vector $\mathbf{T}^{sc}$ for the supercell and a translation vector $\mathbf{T}^{ec}$ characterizing the location of the considered elementary unit cell in the supercell. Inserting the effective force constants into Eq. (1) yields an effective dynamical matrix which is different from the true dynamical matrix. It is also different from the truncated dynamical matrix where only the true force constants within a supercell are considered, because the effective force constants involve also contributions from all the other supercells. However, if the phonon wave vector $\mathbf{q}$ is a vector of the reciprocal lattice of the supercell lattice, i.e., if

$$\mathbf{q}\cdot\mathbf{T}^{sc} = 2\pi n, \quad n \in Z, \tag{3}$$

then the effective dynamical matrix is identical to the true dynamical matrix.[10,11] This becomes obvious when expressing the true dynamical matrix also in terms of $\mathbf{T}^{sc}$ and $\mathbf{T}^{ec}$, yielding

$$\underline{\underline{D}}_{\alpha,\alpha'}(\mathbf{q}) = \sum_{\mathbf{T}^{ec}} \frac{1}{\sqrt{M_\alpha M_{\alpha'}}} \times \left(\sum_{\mathbf{T}^{sc}} \underline{\underline{\Phi}}_{\alpha,\alpha'}(\mathbf{T}^{sc}+\mathbf{T}^{ec})\, e^{i\mathbf{q}\mathbf{T}^{sc}} \right) e^{i\mathbf{q}\mathbf{T}^{ec}}. \tag{4}$$

For the wave vectors $\mathbf{q}$ of Eq. (3) the structure factors $e^{i\mathbf{q}\mathbf{T}^{sc}}$ all attain the value of 1 and the bracket in Eq. (4) is identical to the effective force constant given by Eq. (2). However, if we replace for general $\mathbf{q}$ the bracket in Eq. (4) by the effective force constants (2), then several of the true coupling constants are not weighted by the true structure factors. Nevertheless, close to the wave vectors given by Eq. (3) the effective dynamical matrix is still a better approximation to the true dynamical matrix than the truncated dynamical matrix confined to the true couplings within one supercell. To obtain a good overall representation of the dynamical matrix we therefore can proceed on two alternative lines: First, we can perform calculations for various supercells with different sizes and forms, yielding different effective force constants as different linear combinations of true force constants according to Eq. (2), and then we can try to calculate from the so-obtained set of linear equations as many true coupling constants as possible, including also a sufficiently large number of force constants beyond the range of the supercell, in order to obtain a truncated dynamical matrix with large truncation range. Because this procedure requires an enormous numerical effort we proceeded on an alternative line by evaluating the effective force constants for a simple cubic 54-atom supercell and a body-centered-cubic 64-atom supercell. The effective force constants of the 64-atom supercell yield exact phonon frequencies for the phonon modes for the 32 $\mathbf{q}$ vectors of the Brillouin zone which fulfill Eq. (3) and which we call ''64-atom modes.'' Among these are the modes at the Γ, *R*, *X*, and *M* point (see Fig. 1). On the other hand, the effective force constants of the 54-atom supercell yield exact frequencies for the optical Γ point phonon and for 26 other $\mathbf{q}$ vectors according to Eq. (3) (''54-atom modes''). Now it can be shown that we obtain the correct frequencies for both, the 64-atom modes and the 54-atom modes, when we insert into Eq. (4) the effective 54-atom force constants to the 1, 4, 7, and 10 neighbors and the effective 64-atom force constants to the 2, 3, 5, 6, and 8 neighbors. To calculate the frequencies for a general wave vector $\mathbf{q}$ we therefore replace the brackets in Eq. (4) by these corresponding effective force constants of the 54- and the 64-atom supercell, and we expect to obtain a good interpolation for general wave vectors.

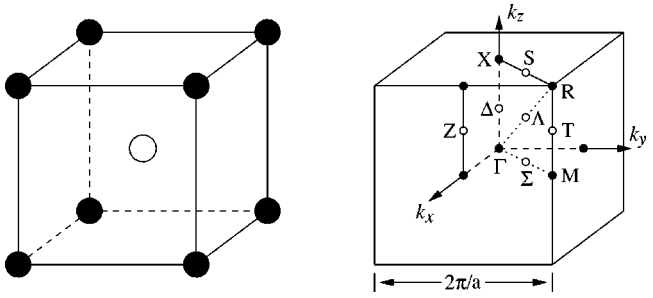

FIG. 1. The *B*2-structure of FeAl (left) and the corresponding Brillouin zone (right).

The calculations were performed within the framework of the density-functional theory in local-density approximation[14,15] and the *ab initio* mixed-basis pseudopotential method[16] for which recently a highly efficient and accurate computer code has been developed.[17] In the mixed-basis method the wave functions are represented by a basis set of plane waves supplemented by five localized *d* orbitals per transition-metal atom. The localized orbitals are constructed in such a way that there is no overlap of orbitals between neighboring atoms, and this allows a simple and accurate calculation of forces. In contrast to the former version of the method,[16] the new code[17] fully takes into account the asphericity of the local part of the pseudopotential when calculating the Hamiltonian matrix elements involving the localized orbitals, and this improves the accuracy of the total energies and especially of the forces.[17] The calculations were performed at the experimental lattice constant $a_0 = 2.909$ Å.[18] We expect that all phonon frequencies would be scaled by a constant factor slightly larger than 1 when performing the calculation at our slightly smaller theoretical lattice constant of $a_0 = 2.822$ Å, in analogy to the behavior of alkali

TABLE I. Frequencies of phonons (in THz) at the Γ, *X*, *R*, and *M* point of the Brillouin zone of *B*2-FeAl. The letters A, O, L, and T stand for acoustic, optic, longitudinal, and transversal. The data of column ''conv.'' (for ''converged'') were obtained for $E_{pw}=30$ Ry and for 364 equivalent *k* points; those of the next two columns for $E_{pw}=12.5$ Ry and for 56 equivalent *k* points. The last column gives the relative differences between the data of the two preceding columns. The experimental data were obtained by inelastic neutron-scattering experiments at room temperature.[20]

Phonon	Expt.	Conv.	ΔE	$\mathbf{F}_i$	Diff.
Γ-O	9.7	9.5	9.60	9.60	—
R-A	6.0	5.8	5.53	5.53	—
R-O	9.7	9.7	9.66	9.65	−0.1%
X-TA	6.3	6.3	6.37	6.40	+0.5%
X-LA	6.3	6.5	6.68	6.72	+0.6%
X-TO	8.1	8.0	8.06	8.07	+0.1%
X-LO	8.6	9.1	9.11	9.11	—
M-LA	2.9	3.1	3.06	3.08	+0.6%
M-TA	7.3	7.6	7.66	7.66	—
M-TO	8.3	7.9	8.06	8.03	−0.4%
M-LO	10.9	10.5	10.66	10.65	−0.1%

metals.[9] The plane-wave cutoff was $E_{pw}=12.5$ Ry, and for the sampling of the Brillouin zone *k*-point meshes according to Chadi and Cohen[19] were used corresponding to 56 equivalent *k* points in the irreducible part of the first Brillouin zone of the elementary unit cell of FeAl. For the frozen-phonon calculations the results were in addition fully converged with respect to E_{pw} and to the number of *k* points.

In the frozen-phonon calculations we determined the change ΔE in total energy and the restoring forces $\mathbf{F}_i$ on the atoms when displacing the atoms according to a snapshot of the atom movement in a normal mode as function of the displacement amplitude. Then fifth- and sixth-order polynomials were fitted to $\mathbf{F}_i$ and ΔE in order to account for anharmonic effects. It thereby turned out that the derivative of the polynomial for ΔE with respect to the displacement amplitude reproduced more or less exactly the calculated forces as function of the displacement amplitude, which serves as a consistency check of our methods to calculate total energies and forces. The eigenfrequencies were calculated from the coefficients of the linear and the quadratic terms of the polynomials, respectively. The results for various high-symmetry points of the phonon Brillouin zone (Fig. 1) are shown in Table I. Again it becomes obvious from the last column of Table I that the results for the frequencies as obtained from the total-energy calculations and from the force calculations are nearly identical. Please note that except for the *R*-*A* phonon the data from calculations with $E_{pw}=12.5$ Ry and 56 equivalent *k* points are already well converged. There is a good overall agreement between theoretical and experimental frequencies, with a mean deviation of about ±0.2 THz and a maximum deviation of 0.5 THz for the *X*-LO phonon.

For the calculation of the force-constant matrix it can be shown by symmetry arguments that for the *B*2 structure of FeAl all effective force constants within the supercell may be determined by just two calculations, once with a single Fe and once with an Al atom $(\alpha,\mathbf{T}^{ec}=0)$ displaced in an arbitrary Carthesian direction. For a given displacement $\mathbf{u}_\alpha$ of

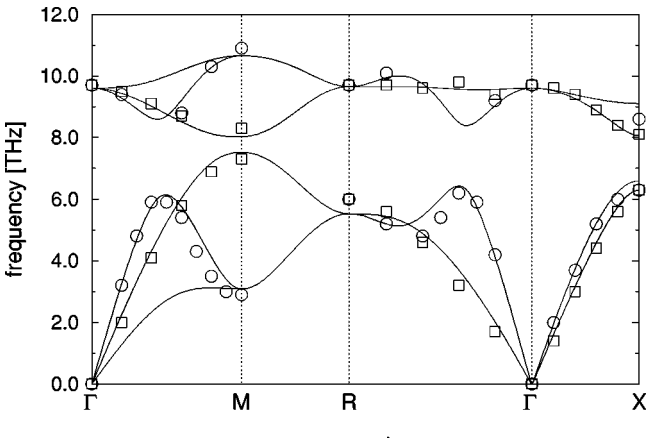

FIG. 2. Theoretical phonon-dispersion curves of FeAl (full lines). The circles (squares) represent the results from inelastic neutron scattering for the longitudinal (transversal) modes at room temperature.

this atom the matrix of the effective force constants was obtained from the forces $\mathbf{F}_{\mathbf{T}^{ec}\alpha'}$ on the basis atoms α' in the primitive unit cell $\mathbf{T}^{ec}$

$$[\Phi^{eff}_{\alpha,\alpha'}(\mathbf{T}^{ec})]_{mn}=-\frac{\partial(\mathbf{F}_{\mathbf{T}^{ec}\alpha'})_n}{\partial(\mathbf{u}_\alpha)_m}=-\frac{(\mathbf{F}_{\mathbf{T}^{ec}\alpha'})_n}{(\mathbf{u}_\alpha)_m}, \qquad (5)$$

where we assumed the harmonic approximation for the last part of Eq. (5). To account for anharmonic effects, the effective force constants were evaluated for different amplitudes of the displacements.

Figure 2 represents the calculated phonon spectrum along high-symmetry lines in the Brillouin zone, together with experimental data obtained at room temperature from inelastic neutron-scattering experiments (details of the neutron-scattering experiments will be given elsewhere).[20] There is a good overall agreement, with all crossings of the dispersion curves described correctly. The slight deviation for the acoustical *R* mode results in part from the fact that at this wave vector the electronic structure calculation is not yet totally converged for $E_{pw}=12.5$ Ry and 56 equivalent *k* points (the converged frozen-phonon frequency is about 0.3 THz higher; see Table I). It should be noted that very similar dispersion curves are obtained when calculating the effective

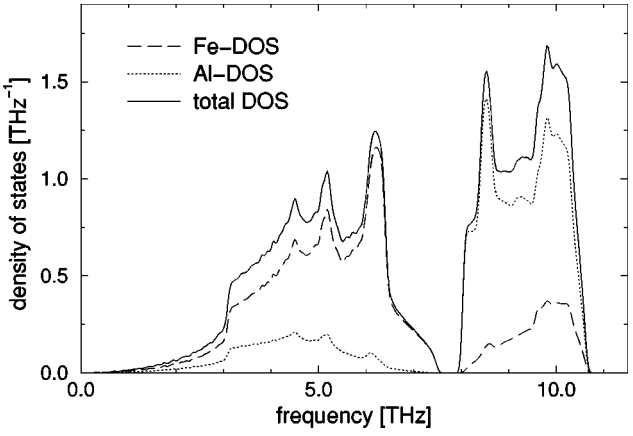

FIG. 3. Theoretical total and partial phonon density of states for *B*2-FeAl.

dynamical matrix exclusively from the effective couplings of the 54-atom supercell or from those of the 64-atom supercell (also the results obtained from a simple-cubic 16-atom supercell are surprisingly close). As in Fe_3Si, but in contrast to β-Ti (Ref. 21) there are no pronounced phonon anomalies which would strongly promote the diffusion of vacancies via nearest-neighbor jumps. The phonon density of states is shown in Fig. 3. As in the case of Fe_3Al,[22,23,1] there is a high frequency part which originates primarily from the low-mass Al atoms and which is separated from the low-frequency part which originates mainly from the high-mass Fe atoms. At low and intermediate temperatures the entropy is dominated by the low-frequency Fe vibrations and therefore the vacancy formation entropy (or, more precisely, the defect entropy parameter[24]) resulting from the change of the vibrational entropy when removing an atom from the system is expected to be larger for an Fe atom than for an Al atom.

The authors are indebted to G. Vogl and B. Sepiol for providing us with the neutron-scattering data prior to publication and to G. Vogl for a critical reading of the manuscript.

[1] L. Anthony, J. K. Okamoto, and B. Fultz, Phys. Rev. Lett. **70**, 1128 (1993); L. Anthony, L. J. Nagel, J. K. Okamoto, and B. Fultz, *ibid.* **73**, 3034 (1994).

[2] A. van der Walle, G. Leder, and U. V. Waghmare, Phys. Rev. Lett. **80**, 4911 (1998).

[3] H. R. Schober, W. Petry, and J. Trampenau, J. Phys.: Condens. Matter **4**, 9321 (1992).

[4] O. G. Randl, G. Vogl, W. Petry, B. Hennion, B. Sepiol, and K. Nembach, J. Phys.: Condens. Matter **7**, 5983 (1995).

[5] J. Mayer, C. Elsässer, and M. Fähnle, Phys. Status Solidi B **191**, 283 (1995).

[6] W. Frank, U. Breier, C. Elsässer, and M. Fähnle, Phys. Rev. Lett. **77**, 518 (1996).

[7] V. Schott and M. Fähnle (unpublished).

[8] P. Staikov, A. Kara, and T. S. Rahman, J. Phys.: Condens. Matter **9**, 2135 (1997).

[9] W. Frank, C. Elsässer, and M. Fähnle, Phys. Rev. Lett. **74**, 1791 (1995).

[10] G. Kresse, J. Furthmüller, and J. Hafner, Europhys. Lett. **32**, 729 (1995).

[11] K. Parlinski, Z. Q. Li, and Y. Kawazoe, Phys. Rev. Lett. **78**, 4063 (1997).

[12] K. Kunc, in *Electronic Structure, Dynamics, and Quantum Structured Properties of Condensed Matter*, edited by D. T. Devreese and P. van Camp (Plenum, New York, 1995), p. 227; S. G. Louie, *ibid.*, p. 335.

[13] S. Baroni, P. Giannozi, and A. Testa, Phys. Rev. Lett. **58**, 1861 (1987).

[14] W. Kohn and L. J. Sham, Phys. Rev. **140**, A1133 (1965).

[15] J. P. Perdew and A. Zunger, Phys. Rev. B **23**, 5048 (1981).

[16] S. G. Louie, K.-M. Ho, and M. L. Cohen, Phys. Rev. B **19**, 1774 (1979); C. Elsässer, N. Takeuchi, K. M. Ho, C. T. Chan, P. Braun, and M. Fähnle, J. Phys.: Condens. Matter **2**, 4371 (1990).

[17] B. Meyer, C. Elsässer, and M. Fähnle (unpublished).

[18] H. J. Leamy, E. D. Gibson, and F. X. Kayser, Acta Metall. **15**, 1827 (1967).

[19] D. J. Chadi and M. L. Cohen, Phys. Rev. B **8**, 5747 (1973).

[20] W. Bührer, M. Zolliker, and G. Vogl, Annual Report (1995), Labor für Neutronenstreuung, ETH Zürich and Paul Scherrer Institut, Report No. LSN-181 (unpublished), p. 51; p. 52; W. Bührer, M. Zolliker, B. Sepiol, and G. Vogl (unpublished).

[21] W. Petry, A. Heiming, J. Trampenau, and G. Vogl, Defect Diffus. Forum **66-69**, 157 (1989); W. Petry, A. Heiming, J. Trampenau, M. Alba, C. Herzig, H. R. Schrober, and G. Vogl, Phys. Rev. B **43**, 10 933 (1991).

[22] I. M. Robertson, J. Phys.: Condens. Matter **3**, 8181 (1991).

[23] E. Kentzinger, M. C. Cadeville, V. Pierron-Bohnes, W. Petry, and B. Hennion, J. Phys.: Condens. Matter **8**, 5535 (1996).

[24] M. Fähnle, G. Bester, and B. Meyer, Scr. Mater. **39**, 1071 (1998); J. Mayer and M. Fähnle, Acta Mater. **45**, 2207 (1997).